

Column adsorption desorption behavior of cationic dyes by Moroccan clay

A. Bennani Karim^{1,2}, B. Mounir¹, M. Hachkar¹, M. Bakasse³ and A. Yaacoubi².

¹ The team of Analysis, Checks and Environment, high School of Technology, Cadi Ayyad University, Safi, Morocco.

² The team Environmental and Experimental Methodology, Laboratory of Organic Applied Chemistry, Faculty of the Sciences Semlalia, Cadi Ayyad University Marrakech, Morocco.

³ The team of Analysis of the Microphones Polluting Organic, Faculty of the Sciences, Chouaib Doukkali University El jadida, Morocco.

* Corresponding Author. E-mail: asmaabennani@yahoo.fr; Tel: (+212661312672)

Received August 03, 2017; accepted December 09, 2017; published December 30, 2017
Copyright © 2017 by authors and Scientific Research Publishing Inc.

Abstract

The adsorption using continuous fixed bed study was carried out by using Moroccan clay as adsorbent for the removal of BR46 and MB dyes. The effect of flow rate, influent dyes concentration and bed depth was studied. It was found that breakthrough time decreases with increasing initial dye concentration (775 - 552 min for BR46, 580 to 420 min for MB) and flow rate (410- 45 min for BR46, 255- 37.5 min for BM), but it increases with rising bed height (267- 580 min for MB, 435- 775 min for BR46). The Bohart-Adams model's and its BDST rearranged one, were implemented to the dynamic adsorption process initial part, to evaluate the fixed-bed column performances. The Clark model was applied to predict the breakthrough curves in the upper range of concentration. And so a good representation of experimental curves in a large domain of concentration is obtained for all used models. This approach in the modeling clean-up process has permitted to put in evidence the complementarity of the used models. The study is achieved by the desorption test. 11% and 7% was retained for the BR46 and MB. This study highlighted the natural clay feasibility as a promising economical adsorbent.

Keywords

Adsorption, Moroccan clay, BR46 and BM dyes adsorbates, dynamic reactor, adsorption modeling, desorption.

1. INTRODUCTION

In industrial waste streams, dyes are among the most common visible pollutants causing environmental and health problems. In addition to the conventional methods (including physical, chemical and biological) used in the treatment of these waste waters [1,2], alternative approaches have been explored [1,3,4]. This mainly concerns the dyes adsorption on natural materials (mineral or vegetal), as low cost waste waters cleanup [5]. The large literature devoted to this topic has revealed an interesting potential of such

process for the treatment of industrial effluents containing synthetic dyes. Both batch and fixed-bed modes were used. Particularly, the clay use as adsorbent has been successful in overlooking the disposal of cationic dyes [6- 8]. Especially, in our previous works [8, 9], it was found that the Moroccan clay of Safi has a PZC of 9.5 [8], a significant potential to remove textile dyes of Basic Red 46 (BR46) [8] and Methylene Blue (MB) [9]. The removal of dye in batch mode was studied. First, the composition of the adsorbent material was determined by using different spectral techniques: FTIR, and X-ray fluorescence XRD.

Physical properties surface area (BET surface area including the outer surface, the total pore volume and the distribution of the average pore size) were also determined. And then batch BR46 and MB dyes removal study concluded the dependence on the physical properties and chemical composition of the adsorbent, that the adsorption kinetics is better described by the pseudo-second-order model and the adsorption equilibrium is better described by the Langmuir isotherm. However, it was found that the Freundlich model was also valid for the description of the complex process of the BR46 and MB adsorption [8, 9]. On the other hand, this study has evidenced that the adsorption process occurs in two steps: the first one is relatively rapid and the second one is slow and asymptotic. But, it has not demonstrated the changes caused by desorption. Although the results involving the use of Moroccan clay to dyes removal are promising, there is still a need for a better understanding of these results by the clay bed adsorption. In the present paper, we'll extend and complete our previous work to column adsorption desorption studies. It concerns especially the study of the fixed-bed adsorption desorption of the BR46 and MB dyes onto the clay of Safi (Morocco) mixed with sand to avoid clogging. To optimize the performances of the filter, the height of the adsorbent bed, the flow rate and the initial dye concentration will be taken as experimental variables. Dynamic experiments will be performed to obtain dyes breakthrough curves through a fixed-bed packed with raw Moroccan clay mixed with sand. Models from the literature such as Bohard-Adams, BDST and Clark models will be implemented to evaluate the performances of fixed-bed column and to predict the breakthrough curves. The study will be achieved by the desorption results using NaCl solution.

2. EXPERIMENTAL

2.1. Adsorbent materiel and dye

The raw clay used in this work was collected from a natural basin in the region of Safi (Morocco), crushed and sieved to particle size < 0.6 mm. Then it was dried at 105°C for 24h and used for further experiments. The dyes used in this study are Methylene Blue (MB) and Basic Red (BR46), which were supplied by High School of Technology and SDI textile company (Safi, Morocco) respectively. Their molar masses are: 319.85 g/mole and 357.5 g/mole respectively.

2.2 Fixed-bed adsorption experiments

Column is Pyrex glass tube with length of 40 cm, 2 cm inner diameter, filled with the amounts of granular clay to be used mixed with sand with 3% as percentage, which were found optimal to avoid clogging. In effect, several experiments have been carried out at different percentage (1%, 2%, 3%, 4%, 5%), 3% was found optimal. For the dyes adsorption experiments, the continuous flow adsorption studies were conducted in the column filled with clay and sand mixtures adsorbent. The sand is previously washed repeatedly to remove excess salt, sieved to a particle size between 0,5 and 1 mm, whereas the clay is crushed and sieved to a particle size of about 600 microns. The relative clay sand size where near than 1 to obtain uniform dispersion of clay particles. A quantity of clay mixed with sand (3% as sand clay percentage) was packed between a layer of 5 mm size glass beads in order to provide a uniform flow of the solution through the column, a filter paper is placed in the end of the column in order to prevent the escape of the clay to yield the desired bed height of the adsorbent (15- 30 cm) and initial dyes concentrations (160- 260 mg/L). A blank test on the sand only has been done; the results showed that his dyes adsorption is negligible.

Working solutions, at required concentrations, were stored in glass tanks and were pumped into the fixed bed column by a peristaltic pump at constant volumetric flow rate (Fig. 1). The samples of the effluent were collected at regular intervals and analysed by UV-Vis spectroscopy. A spectrophotometer [GBC (Ajax, Ontario) UV/visible 911] was used for the experiments. A linear correlation was established between the dye concentration and the absorbance at $\lambda_{\max} = 532$ nm for the BR46 and $\lambda_{\max} = 666$ nm for the MB when the correlation coefficient r^2 c.a. 1 with a concentration less than 20 mg/L for the BR46 and 24 mg/L for the MB. For analysis of the solutions at higher concentrations, the appropriate dilutions were performed.

The operating parameters studied were the adsorbent mass (bed depth), volumetric flow rate and initial dye concentration. All the experiments were carried out at room temperature ($25 \pm 1^\circ\text{C}$) and pH c.a. 6.5. The reproducibility during mass loss measurements was ensured by repeating the experiments three times under identical conditions and average values are reported. Standard deviations during experiments were found to be within $\pm 5.0\%$. After exhaustion of the Moroccan clay by BR46 and MB at a known concentration as: 210 mg/L, it was necessary to test dye desorption possibility for further use of the clay. Aqueous NaCL (0,5M) were used for the desorption test on the exhausted (saturated) clay. The shematic diagram is illustrated in Fig 1.

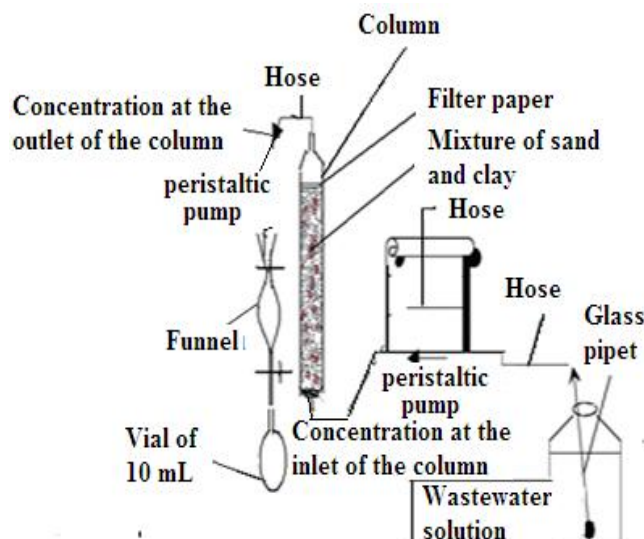


Fig.1. Schematic diagram of laboratory based small column for fixed bed studies

2.3. Operating variables

BR46 and MB cationic dyes solutions were pumped upward through the column at the optimal flow rate obtained using a peristaltic pump until the dye concentration at the outlet of the column becomes almost equal to that of the input. The BR46 and MB dyes solutions at the outlet of the column were collected respectively at regular time intervals.

2.3.1. Effect of flow rate for the BR46, and MB dyes adsorption studies

The Moroccan clay adsorbent of different flow rate (4, 8.5 and 12 mL/min) was placed in separate glass columns: 260 mg/L for the BR46 and MB respectively working standard at pH 5.5 ± 0.2 was percolated through each of the column. The samples from each column were collected at certain time interval and kept for dye analysis.

2.3.2. Bed height of the BR46 and MB dyes adsorption studies

A clay quantity of 2.25; 3; 3.75 and 4.5 g was mixed with 75, 100, 125 and 150 g of sand to provide bed depths of approximately 15 cm, 20 cm, 25 and 30 cm, respectively. 160 mg/L working standard at pH 5.5 ± 0.2 was percolated through each of the column using the appropriate flow rate found. The samples from each column were collected at certain time interval and kept for dye analysis.

2.3.3. BR46 and MB dyes concentration studies

BR46 and MB cationic dyes solutions at concentrations 160, 210 and 260 mg/L and pH of 6.5 were pumped upward through the column at the optimal flow rate obtained. The samples from each column were collected at certain time interval and kept for dye analysis.

2.4. General consideration on column data analysis

The breakthrough curves are a convenient tool to highlight the performances of fixed-bed column. The time for breakthrough appearance and the shape of the breakthrough curve are very important characteristics for determining the operation and dynamic process of a sorption column [10, 11]. The residual concentration (C_t) from the column that reaches about 3% of the influent concentration (C_0) is commonly designed as the breakthrough point. The point where the effluent concentration reaches 95% is usually called the “point of column exhaustion” [12]. In order to ensure the quality of the data, a "blank" sample was prepared and handled in parallel for each adsorption test. The blank test was performed on sand alone. The results showed that the MB and BR46 dyes adsorption onto sand used is negligible.

The breakthrough curve is usually expressed by residual concentration (C_t) or normalized concentration (C_t/C_0) as a function of time for a given bed depth.

The experimental BR46 and MB dyes amount adsorbed per clay unit mass, q_{exp} (mg/g), in the column was calculated using the relationship:

$$q_{exp} = \frac{(C_0 - C_e)}{w} \quad (1)$$

Where C_0 (mg/L) and C_e (mg/L) are the initial and the equilibrium dye concentration in the liquid phase, w (g) is the amount of sorbent.

The effluent volume V (mL) can be calculated as: $V = q_v \cdot t_{total}$

Where t_{total} and q_v are the total flow time (min) and the volumetric flow rate (mL/min)

The value of the total mass of dyes adsorbed, q_{total} (mg), can be calculated as:

$$q_{total} \text{ (mg)} = w \cdot q_{exp}$$

The amount of dyes entering column, m_{total} , is calculated from the following equation:

$$m_{total} \text{ (mg)} = (C_0 \cdot V)$$

V (L) is the effluent volume of solution

The removal percentage of dyes can be obtained from equation: $Y(\%) = (q_t \cdot 100) / m_{total}$

2.5. Fixed-bed desorption experiments

The desorption tests were performed on the saturated sand with a bed height of 20 cm and a dye concentration of 210 mg/L for the blank test using deionized water in the first step and NaCl solution (0,5 mg/ L) in the second step, and then on the mixed sand and clay adsorbent (with a percentage of 3%), saturated with the dyes using deionized water, than NaCl solution (0,5M), to deduce the desorption percentage of MB and BR46 dyes by the adsorbent clay. The dye desorption percentage: %des, can be calculated from the following equation: $\%des = C_{des}/C_i * 100$.

3. RESULTS AND DISCUSSIONS

3.1. BR46 and MB dyes studies in dynamic system

The results of BR46 and MB dyes dynamic adsorption on the mixed sand and clay were presented as breakthrough curves, it showed the loading behaviors of dyes adsorbed from the solution, expressed by residual concentration as a function of time (C_r vs. t).

C_0 and C_r : Initial and Residual dye concentration (mg / L); q_v : Flow rate (mL/min)

3.1.1. Effect of flow rate for the BR46 and MB dyes

To find out the effect of flow rate on the breakthrough curves, adsorption experiments were carried at 4, 8,5 and 12 mL/min. In this process, the initial MB and BR46 dyes concentration and bed height were maintained at 260 mg/L and 20 cm respectively. The effect of flow rate on breakthrough performance at the above operating conditions is shown in Fig.2a.

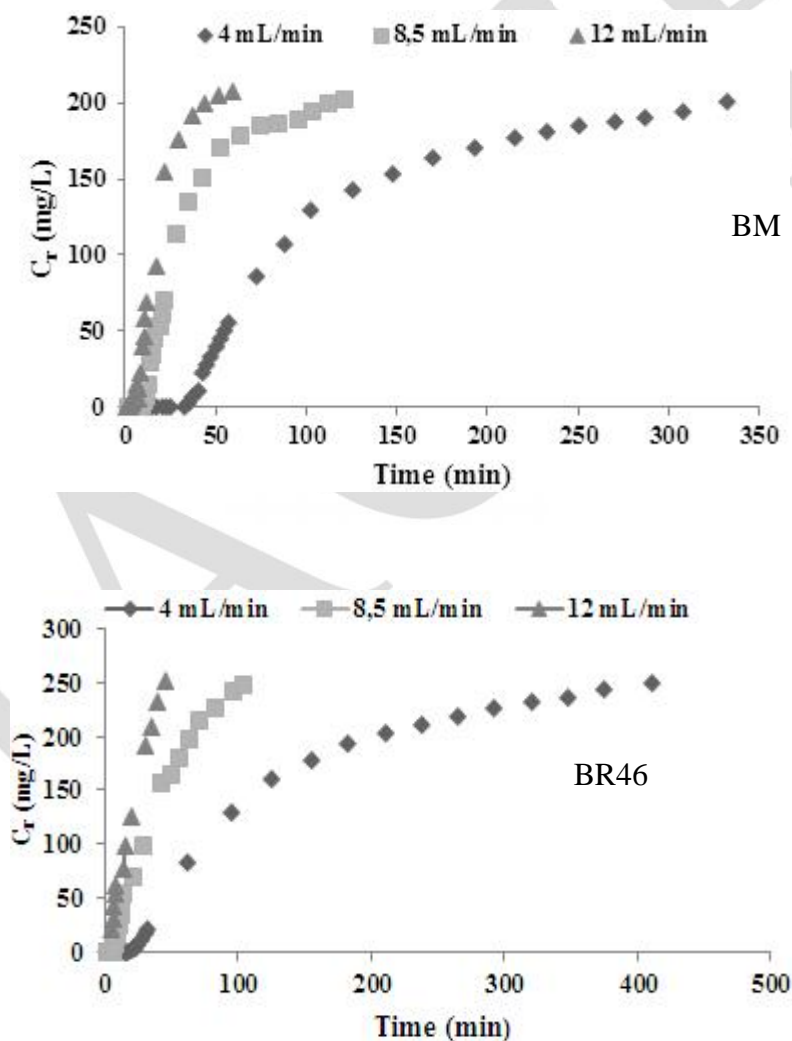


Fig.2a. Breakthrough curves for MB and BR46 adsorption onto clay at temperature = $25 \pm 1^\circ\text{C}$ at different volumetric flow rates (initial dye concentration = 260 mg/L, $Z = 20$ cm).

From this figure, it was observed that the adsorption efficiency was lower at higher flow rate and the adsorbent gets saturated easily at higher flow rates. It can be explained by the fact that at higher flow rate, the external film mass resistance at the adsorbent surface tends

to decrease and the residence time decreases. Hence the saturation time decreases and gives the lower removal efficiency [13]. As indicated in Fig 2a, the breakthrough curves became steeper as the flow rate increased. The lower removal of BR46 and MB in column may be due, as a first approximation, to the shorter residence time of the solute in the column, which does not allow reaching the adsorption equilibrium. In other words, at low flow rate, the diffusion process, which probably controls the sorption, takes place. Hence, the adsorbent needs more time to bond the adsorbate efficiently. The optimum uptake capacity for flow rate of 4, 8.5 and 12 mL/min was found to be 47.34, 30.80 and 21.87 mg/g respectively for the BR46, 28.05; 20.06 and 11.65 mg/g respectively for the MB (Table 1). The removal percentage of the dyes adsorbates follows the same trend.

Figure 2 a shows also that the saturation time is occurred at 410, 103 and 45 min for the BR46, and 255; 98.75 and 37.5 min for the MB when the flow rates were 4, 8.5 and 12 mL/min respectively. Hence, at lower flow rate, the dyes ions have more time to contact with the adsorbent which resulted in higher removal of dyes ions in the fixed bed column. Similar tendency has been found in other similar work [14- 15].

Table 1: Column data and experimental parameters at different initial concentration, bed height and volumetric flow rate, on the adsorption of the MB and BR46 dyes

	C_0 (mg/L)	q_v (mL/min)	Z (cm)	Adsorbent amount (g)	t_{total} (min)	m_{total} (mg)	q_{total} (mg)	q_{exp} (mg/g)	V_{eff} (mL)	Y (%)
BM	160	4	15	2.25	267	171.2	61.51	27.34	1070	35.9
	160	4	20	3	360	230.4	89.25	29.75	1440	38.7
	160	4	30	4.5	580	371.2	159.57	35.46	2320	42.9
	210	4	30	4.5	495	415.8	167.2	37.17	1980	40.2
	260	4	30	4.5	420	436.8	170.91	37.98	1680	39.1
	260	4	20	3	255	267.8	84.15	28.05	1030	31.42
	260	8.5	20	3	98.75	205.4	61.8	20.6	790	30
	260	12	20	3	37.5	117	34.95	11.65	450	29.87
	260	12	20	3	45	245.7	65.61	21.87	945	26.7
BR46	160	4	15	2.25	435	278.4	100.89	44.84	1740	36.2
	160	4	20	3	560	358.4	135.99	45.33	2240	37.9
	160	4	30	4.5	775	496	217.48	48.33	3100	43.8
	210	4	30	4.5	632	531.3	223.50	49.69	2530	42.0
	260	4	30	4.5	552	574.6	231.43	51.43	2210	40.2
	260	4	20	3	410	426.4	142.02	47.34	1640	33.2
	260	8.5	20	3	103	305.76	92.40	30.80	1176	30.21
	260	12	20	3	45	245.7	65.61	21.87	945	26.7
	260	12	20	3	45	245.7	65.61	21.87	945	26.7

3.1.2. Effect of initial BR46 and MB dyes concentration

Effect of initial BR46 and MB dyes concentration was carried out at 160, 210 and 260 mg/L. During these experiments, other parameters like bed height and flow rate were kept constant at 30 cm and 4 mL/min respectively. The sorption breakthrough curves obtained for initial dye concentrations of 160, 210 and 260 mg/L, are given in Fig.2b. As expected, a decrease in the initial MB and BR46 concentration gave an extended breakthrough curves indicating that a higher volume of the solution could be treated. The breakthrough time decreases with increase in inlet dyes concentration as the binding sites became more quickly saturated and the dye loading rate increases. The effect of an appreciable increase in adsorption capacity is presented in Table 1. As the effluents dyes concentration increased from 160 to 260 mg/L, the exhausted time decreased from 775 to 552 min for the

BR46 and from 580 to 420 min for the MB. The uptake of BR46 and MB (q_{exp}) increase from 48.33 to 51.43 mg/g and from 35.46 to 37.98 mg/g respectively. Simultaneously, the removal percentage of BR46 and MB decreases appreciably. At the highest BR46 and MB concentration of 260 mg/L, the mixed adsorbent bed was exhausted in the shortest time (552 min and 420 min respectively), leading to the earliest breakthrough. The treated volume was the greatest at the lowest effluent concentration. These results demonstrate that the change of concentration gradient affects the saturation rate and breakthrough time. This may also be attributed to the high influent dyes concentration providing higher driving force for the transfer process to overcome the mass transfer resistance. Similar tendency has been found in other similar work [15- 17].

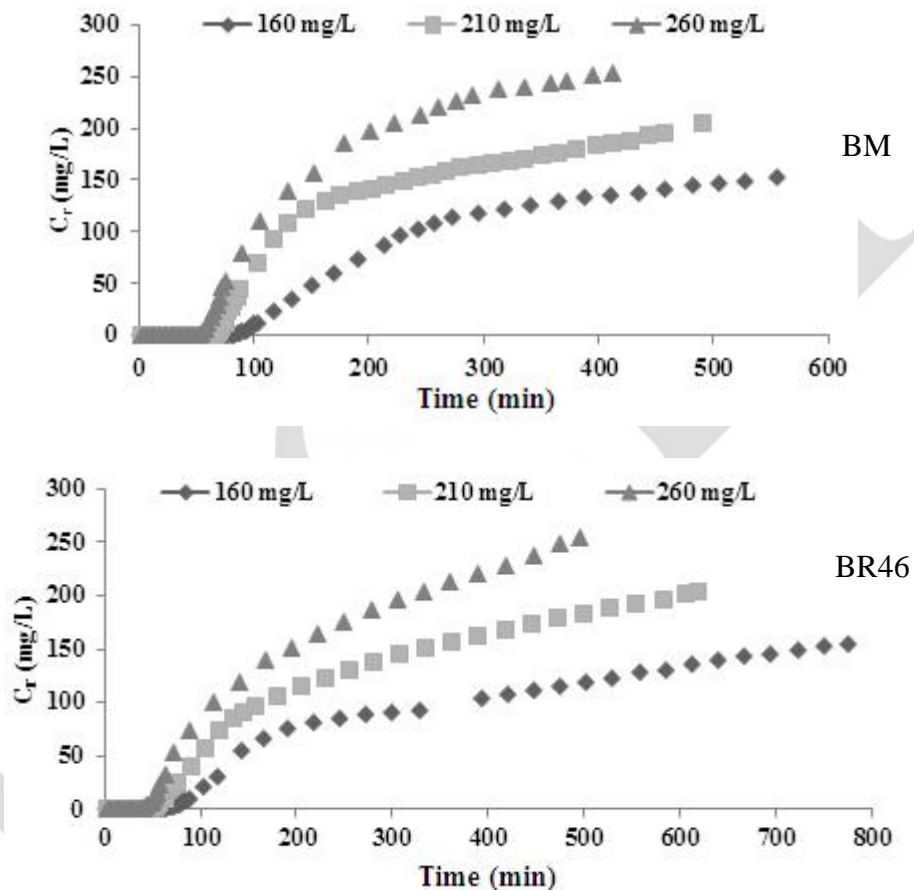


Fig.2b: Breakthrough curves for MB and BR46 dyes adsorption onto clay at temperature = $25 \pm 1^\circ\text{C}$ at different initial dyes concentrations (bed height = 30 cm, $q_v = 4 \text{ mL/min}$)

3.1.3. Effect of bed height

In order to evaluate the effect of bed height on the breakthrough curve, the initial adsorbate concentration and flow rate were maintained at 160 mg/L and 4 mL/min respectively. The obtained breakthrough curves at bed heights of 15, 20, 25 and 30 cm are presented in Fig.2c. Initially, the adsorption was very rapid. This may obviously be attributed to the fact that more amount of sorbent at a given bed heights provides more binding sites for the dye molecules retention. In the next stage of the process, the uptake becomes less effective, it is due to the gradual occupation of these sites. The column is able to accumulate adsorbate even after breakthrough occurs although at a progressively lower efficiency. The bed depth

increased, as well as the exhaustion time (267- 580 min for MB and 435- 775 min for BR46 for dye concentration of 160 mg/L) and consequently, the effluent volume (V_{eff}) increased (Table 1). As shown from Table 1, the removal efficiency of BR46 and MB had an increasing trend in column with the increase in the adsorbent amount. The slope of breakthrough curve decreased with increasing bed depth, which may result in a broadened mass transfer zone [15, 18]. The curve associated to the longer bed (30 cm) tends to be more gradual, meaning the column is difficult to be completely exhausted [19].

On the other side, it's reported in the literature [18] that when the bed height is reduced, axial dispersion phenomena predominate in the mass transfer and reduce the diffusion of the solute, and therefore the solute have not enough time to diffuse into the whole of the adsorbent mass. Similar trends were obtained for adsorption of basic dye using activated carbon and low cost adsorbent [14, 15, 19]

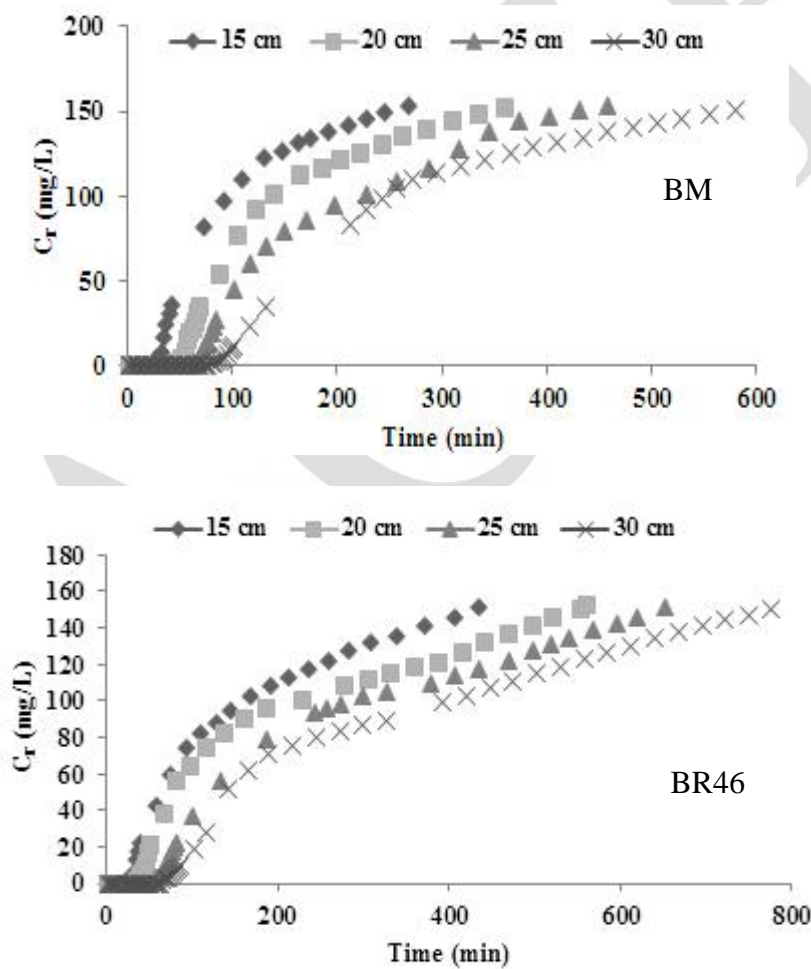


Fig.2c. Breakthrough curves for MB and BR46 adsorption onto clay at temperature = $25 \pm 1^\circ\text{C}$ at different bed heights onto clay (concentration = 160 mg/L, $q_v = 4 \text{ mL/min}$).

3.2. Adsorption modeling

We have concluded in our previous work on the study of the removal of BR46 and MB dyes in batch mode [8- 9] that the adsorption takes place in two phases: the first one corresponds to a rapid adsorption phase and the second one corresponds to a progressive fixation. The obtained results showed that the adsorption kinetics is better described by the pseudo-second-order model. The previous study also concluded that the adsorption equilibrium is mainly described by the Langmuir isotherm (correlation coefficient c.a. 0.99) without excluding the validity of the model of Freundlich (correlation coefficient c.a. 0.96).

In the literature, the modeling approach in the dyes dynamic adsorption process is almost systematically adopted. However, the used models are numerous and sometimes redundant [20]. Therefore, the experimental results can be decisive in the choice of appropriate models. So, according to our previous kinetic and thermodynamic results and to the shape of breakthrough curves, the Bohart-Adams simple model and its derived one, the Bed Depth Time Service (BDST) model, seems more favorable, and will be implemented, to determine the performances of the fixed-bed column. Those models will be applied particularly in the initial part of the dynamic process, when the concentration in the effluent is lower than $0.15 C_i$ [21]. Otherwise, the breakthrough curves will be predicted by using the Clark model, especially in the upper range of concentration.

Both of the two models, i.e. Bohart- Adams and Clark models should be able to give complementary modeling capabilities for the whole complex process of the BR46 and MB adsorption.

3.2.1 Evaluation of the fixed-bed characteristics and performances

3.2.1.1 Application of the Bohart-Adams model

Bohart- Adams model which was originally used for gaseous application has been transposed for liquid applications; its suitability is in low concentration regions and when the speed of adsorption is limited by mass transfer [16], it assumes that the adsorption rate is proportional to both the residual capacity of the adsorbent and the concentration of the adsorbed species [22, 23]. The bed is assumed to be homogeneous and gradients occur only in the axial direction. This model can be expressed in his simplified expression, after the resolution of the governing equations as [24]:

$$\text{Where: } \ln\left(\frac{C_0}{C_b} - 1\right) = K_{BA} N_0 \frac{Z}{v} - K_{BA} C_0 t \quad (2)$$

C_0 : the inlet dye concentration (mg.L⁻¹)

C_b : the breakthrough concentration (mg.L⁻¹)

K_{BA} : the Bohart-Adams rate constant (L/mg min)

t : time (min)

N_0 : the sorption capacity of the adsorbent per unit volume of the bed (mg/L)

Z : total bed depth (cm)

v : linear velocity (cm/min)

The Bohart-Adams model is used for the description of the initial linear part of the breakthrough curve ($C_b \ll C_0$). So, his expression is reduced to:

$$\ln\left(\frac{C}{C_0}\right) = K_{BA} C_0 t - K_{BA} N_0 \frac{Z}{v} \quad (3)$$

From this equation, values describing the characteristic operational parameters of the column can be determined from a plot of $\ln C/C_0$ versus time using the nonlinear regressive method.

For all breakthrough curves, respective values of N_0 , and k_{BA} were calculated from the slope and the intercept of the first linear parts of the figure 3a and presented in Table 2 with the corresponding correlation coefficients at all the inlet BR46 and MB dyes concentrations and bed height studied.

Table 2: Bohart-Adams model parameters at different initial dye concentration and bed heights, adsorption capacities derived from the BDST model at $C_i = 160$ mg/L for the MB and BR46

Bohart and Adams Model ($q_v = 4$ mL/min)						BDST model ($C = 160$ mg/L)					
C_0 (mg/L)	Z (cm)	N_0 (mg/L)	K (L/mg.min)	R^2		$C_t/C_0 = 3(\%)$		$C_t/C_0 = 10 (\%)$		$C_t/C_0 = 20(\%)$	
						K (L/mg.min)	N_0 (mg/L)	K (L/mg.min)	N_0 (mg/L)	K (L/mg.min)	N_0 (mg/L)
BM	160	15	608.12	0.0012	0.97	0,0013	801.27	0,00085	1036.73	0,0006	1266.88
	160	20	622.92	0.0012	0.98						
	160	30	775.79	0.00097	0.97						
	210	15	629.14	0.001	0.98						
	210	20	679.77	0.001	0.95						
	210	30	804.93	0.001	0.97						
	260	15	631.52	0.0009	0.95						
	260	20	710.82	0.0008	0.94						
	260	30	839.33	0.0007	0.95						
BR46	160	15	618.15	0.0013	0.99	0.0012	643.62	0.00075	863.60	0.00047	1012.28
	160	20	657.32	0.001	0.95						
	160	30	753.34	0.0004	0.94						
	210	15	662.10	0.001	0.98						
	210	20	696.97	0.0008	0.98						
	210	30	788.69	0.0006	0.96						
	260	15	688.85	0.0008	0.98						
	260	20	709.39	0.0007	0.96						
	260	30	803,02	0.00057	0.95						

The adsorption capacity, q_0 (mg/g) is calculated as:

$$q_0 = \frac{N_0 Z S}{w} \quad (4)$$

Where:

N_0 : adsorption capacity of the adsorbent per unit volume

Z : bed height (cm)

S : column section (cm²)

w : adsorbent amount (g)

After applying Eq. (3) to the experimental data at various initial dyes concentrations and bed heights, a linear relationship between $\ln C/C_0$ and t was obtained for the relative low residual dyes concentration breakthrough. For all breakthrough curves ($R^2 > 0.900$). Respective values of N_0 , k_{AB} called also: the mass transfer coefficient, were calculated from the $\ln C/C_0$ versus t plots at all initial dyes concentrations and bed heights studied, the results are presented in Table 2 together with the correlation coefficients. The values of kinetic constant was influenced by initial dyes concentrations and decreased by increasing C_0 .

This showed that the overall system kinetics is dominated by external mass transfer in the initial part of adsorption in the column [24].

As expected, the maximum adsorption capacity (N_0), or the saturation concentration, increased with increasing the inlet dyes concentration. The Bohart-Adams model provides a simple and comprehensive approach to conduct and evaluate the sorption-column test. However, its validity is limited to the range of conditions used [10, 13].

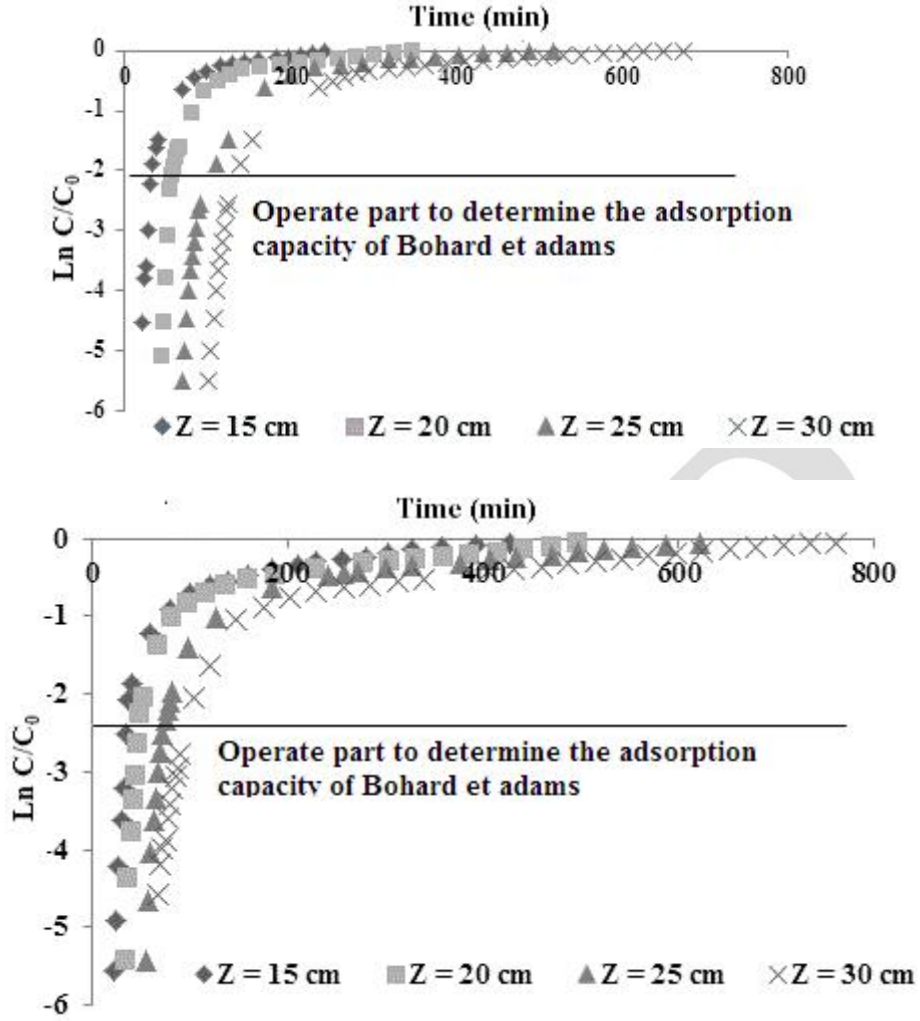


Fig. 3a. MB and BR46 dyes curves at different bed heights ($q_v : 4 \text{ mL/min}$, $m_{\text{clay}} = 3\% m_{\text{sand}}$, $T : 25^\circ \pm 2^\circ \text{C}$) of $\text{Ln}(C/C_0) = f(t)$ for an initial dye concentration of 160 mg/L

3.2.1.2. Application of the Bed-Depth Service Time (BDST) model

Bohart and Adams [25] developed an equation to describe the relationship between service time (t) and bed height (Z) for a fixed-bed adsorber. Service time is referring to time spent by the adsorption column to reach the breakthrough point with specific saturation percentage, and it was related to the adsorption operating conditions (eq. (2)). It gives an idea on the column efficiency under constant operations for achieving a desired breakthrough level. Eq. (2) can be rearranged according to the expression type:

$t = az + b$:

$$t_b = \frac{N_0 Z}{C_0 V} - \frac{1}{K C_0} \ln\left(\frac{C_0}{C_t} - 1\right) \quad (5)$$

Where C_t is the breakthrough dye concentration (mg/L), N_0 the bed sorption capacity (mg/L), V is the linear velocity (cm/min), and K is the rate constant (L/mg. min). The column service time was selected as time when the normalized concentration, C_t/C_0 reached 0.03. The initial concentration C_0 , and flow velocity q_v , may be assumed to be reasonably constant during the column operation. From iso-removal lines: the plots of time

(t_b) versus bed height (Fig. 3b), the main parameters of the Bohart- Adams model can be calculated. Iso-removal lines were plotted for different bed heights (15, 20, 25 and 30 cm), at concentration ratios: $C_t/C_0 = 0.03$, $C_t/C_0 = 0.1$ and $C_t/C_0 = 0.2$. The breakthrough time at desired breakthrough concentrations exhibit almost linearity with bed depth. The calculated constants for the BDST model for the adsorption of BR46 and MB are presented in Table 2. From the respective linear equation, the necessary bed height for a pre-selected time period can be directly calculated until a defined breakthrough concentration [26]. As expected, maximum adsorption capacity (N_0) increased with increasing the ratio: C_t/C_0 BR46 and MB concentration, but the values of k decreased with increasing C_t/C_0 . This once again confirms the fact that the overall kinetics system was dominated by external mass transfer in the initial part of adsorption in the column (experiments carried out at $C_0 = 160$ mg/L).

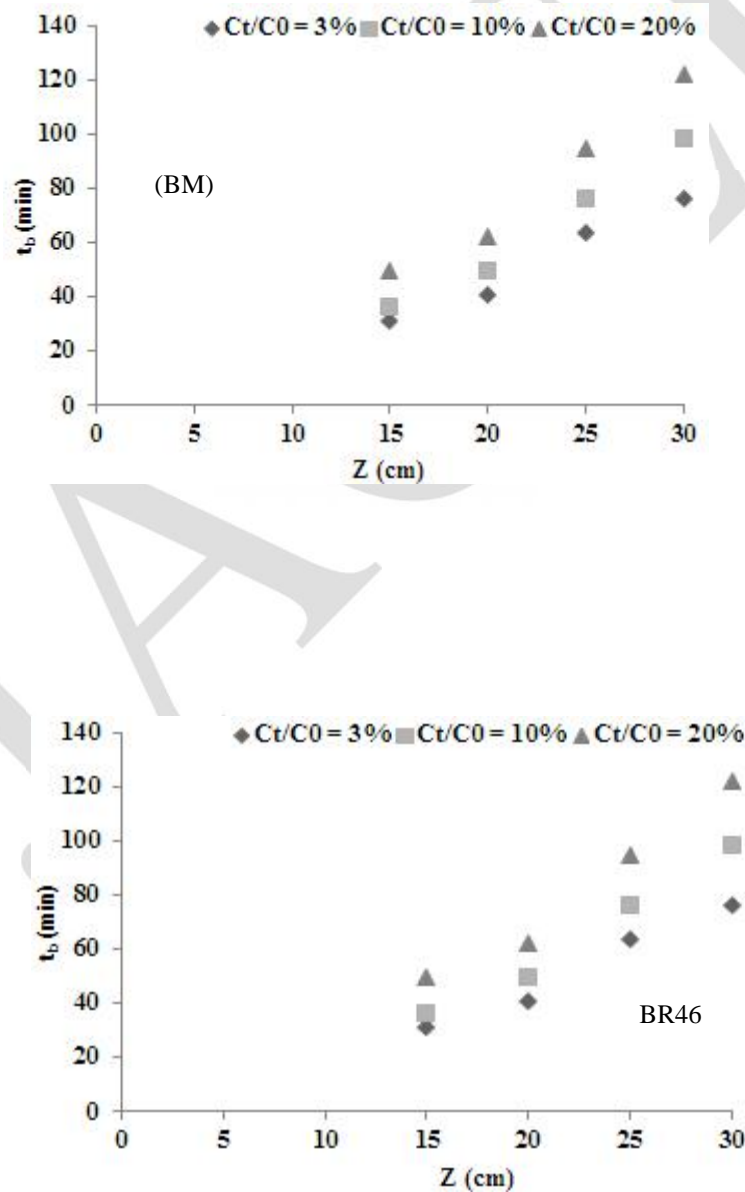


Fig.3b. MB and BR46 dyes evolution of the breakthrough time vs. Z for the BDST model at different bed heights and for different concentration ratios ($q_v : 4$ mL/min, $m_{clay} = 3\%$ m_{sand} , $T : 25^\circ \pm 2^\circ C$)

3.2.2. Prediction of the breakthrough curves

Application of the Clark model

The Clark model [24] is considered as a particularly attractive approach to describe dynamic adsorption. Theoretical bases on a mass-transfer concept in combination with the Freundlich adsorption isotherms; this model has a precise analytical solution enabling determination of dynamic adsorption rate constants.

In previous equilibrium studies, it was found that the Freundlich model was valid for the description of BR46 and MB adsorption onto Moroccan clay [8, 9], which permits the use of the Freundlich constant ($n = 4.35$ and 7.14 for the BR46 and MB respectively) to calculate the parameters in the Clark model [27]:

$$C = \left[\frac{C_0^{n-1}}{1 + Ae^{-rt}} \right]^{1/n-1} \quad (6)$$

The values of A and r can be obtained from the following linearized equation (Fig 4a):

$$\ln \left[\left(\frac{C_0}{C} \right)^{n-1} - 1 \right] = \ln A - rt \quad (7)$$

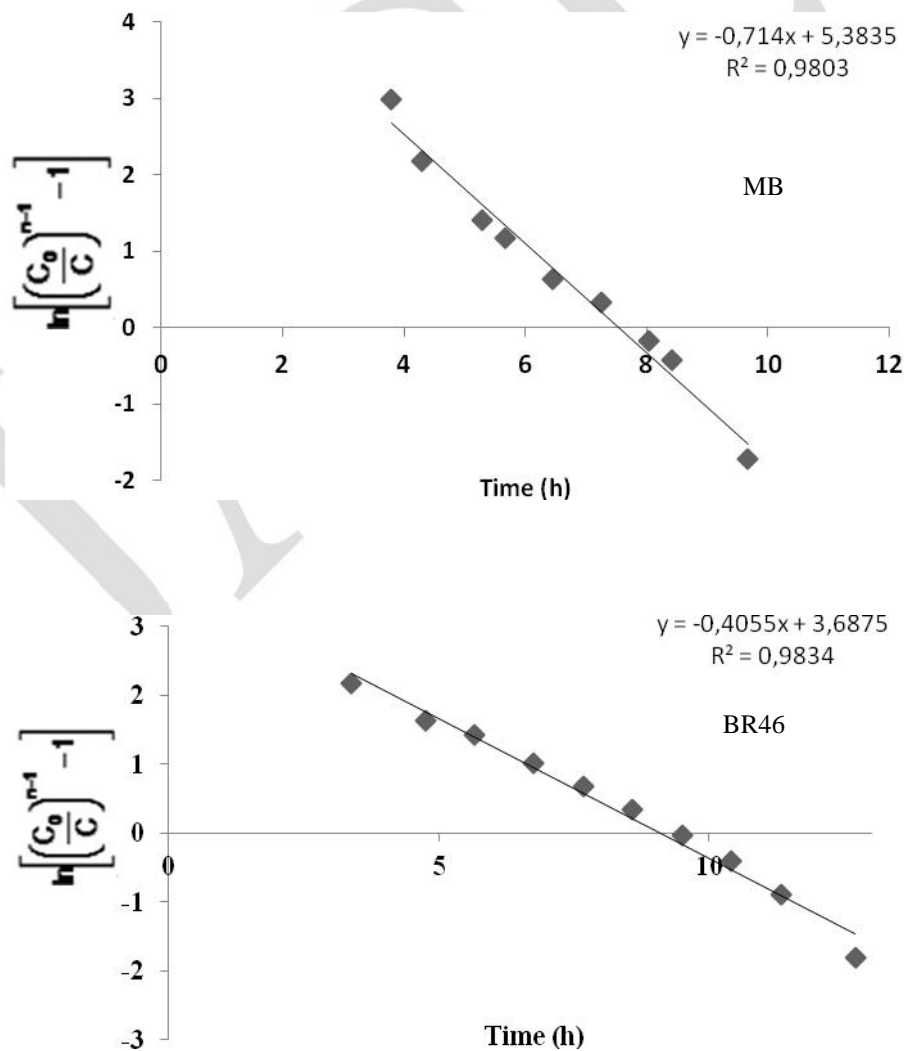


Fig. 4a. MB and BR46 dyes determination for the Clark model at $Z = 30$ cm and $q_v = 4$ mL/min of A and r parameters ($C_0 = 160$ mg/L)

By plotting $\ln \left[\left(\frac{C_0}{C} \right)^{n-1} - 1 \right]$ versus time using nonlinear regressive analysis (Fig. 4a). The Clark model parameters (A and r) can be determined. These parameters are replaced in Equation 6 to calculate the Clark concentration. The Clark and experimental concentrations representation is shown in Figure 4b. The adsorption breakthrough could be well described by the Clark model at the ratios of C_t/C_0 higher than 0.4 (Fig. 4b). In the present study, we used this model for the full range of studied dye concentration. Fitting of the experimental and modeled breakthrough curves, indicates an excellent applicability of the Clark kinetic equation at the ratios of C_t/C_0 higher than 0.4, after about 3,5 hours of flow for BR46 and about 2,5 hours for the MB.

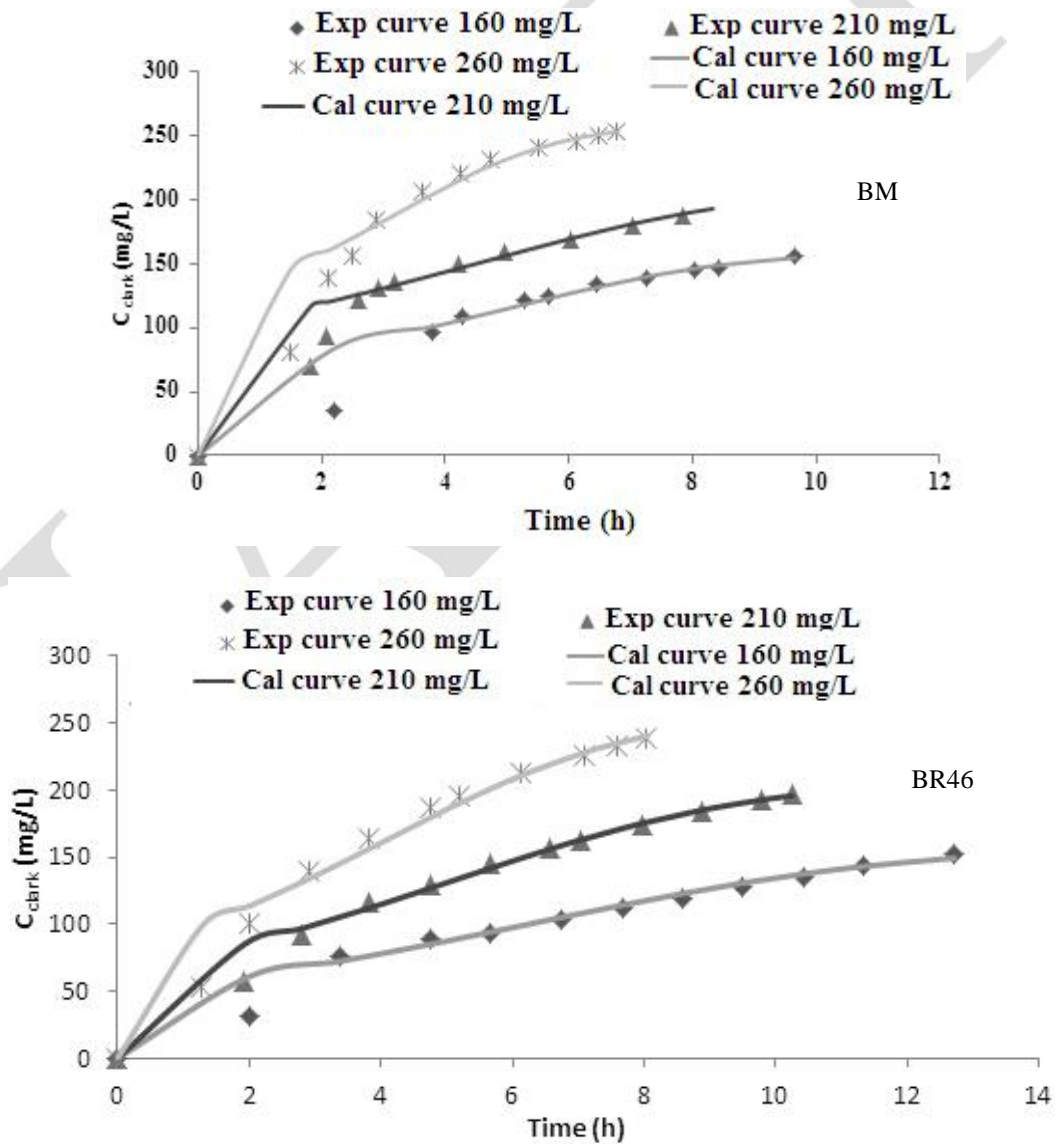


Fig. 4b. MB and BR46 dyes breakthrough curves prediction: experimental data (dashed lines) and calculated data (continuous lines) for different initial dye concentrations,

3.2.3. Focus on the modeling study

In our modeling investigation, we have opted for a small number of models capable of describing the adsorption process of the BR46 and MB dyes and to determine the performances of the used fixed-bed column. In a concentration range, the Bohart-Adams, BDST and Clark models showed good complementarity. Both performances of the column and breakthrough curves are obtained with good correlation with the experimental data. The testing of experimental breakthrough curves by Clark kinetic equation has shown excellent fitting of experimental points with modeled curves, especially at the ratios of C_t/C_0 higher than about 0.4.

3.3. Dynamic BR46 and MB dye desorption

Desorption process gives an idea about the interaction type between the sorbate and the sorbent, regeneration possibility and thus reversibility phenomena.

Recovery of adsorbates material dyes as well as the adsorbent regeneration is an important process in wastewater treatment [28]. The adsorbent clay which gets exhausted on continuous column studies using a peristaltic pump through the mixed adsorbent (sand and clay mixture), is saturated with BR46 or MB respectively. At this point, (saturation point), the influent concentration (dye solution pouring into the column) is equal to the concentration of effluent (dye solution coming out from the column). Therefore, the recovery of the adsorbed material (dyes) as well as regeneration of the adsorbent clay becomes quite necessary.

The exhausted sand and clay column which was loaded with BR46 and BM respectively at 210 mg/L, and a bed high of 20 cm was regenerated with deionized water in the first step, and with NaCL (0,5M) solution in the second step until the concentration at the outlet becomes zero. 1600 mL and 2040 mL of Deionized water was added firstly to the exhausted BR46 and BM sand and clay column respectively till the concentration becomes zero, 1330 mL and 1272 mL of NaCL (0,5M) solution was added secondly to these exhausted columns (by BR46 and BM respectively) of sand and clay till the concentration remains 0 (Figure 5). Before that, The desorption tests were performed on the saturated sand to eliminate the unadsorbed MB and BR46 respectively on the sorbent surface at bed height of 20 cm and a dyes BR46 and BM concentration of 210 mg/L respectively for the blank tests until the concentration at the outlet becomes zero, 1250 mL and 1000 mL of Deionized water was added firstly to the exhausted BR46 and BM sand column respectively till the concentration becomes zero, 420 mL and 280 mL of NaCL (0,5M) solution was added secondly to these exhausted columns of sand (by BR46 than BM) till the concentration remains 0 (Figure 5; Table 3).

Table 3: Desorption percentage of MB and BR46 dyes.

	Desorption percentage using ultrapure water %		Desorption volume using ultrapure water (mL)		Desorption percentage using NaCl %		Desorption volume using NaCL (mL)		Total desorption percentage (ultrapure deionized water than NaCl%		Desorption volume deionized water than NaCl (mL)	
	BM	BR46	BM	BR46	BM	BR46	BM	BR46	BM	BR46	BM	BR46
Mixed adsorbent desorption	10	13	2040	1600	7	13	1330	1272	17	26	3370	2872
Sand desorption	7	10	1000	1250	3	5	280	420	10	15	1280	1670
Clay desorption	3	3	3040	1850	4	8	1050	850	7	11	1090	1202

All the desorption experiments were carried out at room temperature ($25 \pm 1^\circ\text{C}$), a bed height of 20 cm and exhausted adsorbent dyes concentration of 210 mg/L for the BR46 and the BM respectively. To avoid the maximum error in the results, hoses and filter paper saturated with the adsorbate in the adsorption tests were renewed and other new ones were placed for the desorption tests. The MB and BR46 solutions desorbed at the outlet of the column were collected at regular time intervals and the concentration was measured using a spectrophotometer [GBC (ajax, ontario) UV/visible 911] at 666 and 532 nm respectively. The concentration of solution passing through the columns was monitored continually by collecting manually the samples in volumetric flasks. The curves were constructed as C_{desorbed} vs. time. we can conclude from Figure 5 that the increase of the residual BR46 and MB desorbed concentration after adding NaCl suggest a competitive adsorption between cations of the NaCl solution and the dyes adsorbates [14]. The desorption results of BR46 and BM summarized in Table 3 show a desorption percentage of 11% and 7% for the BR46 and the BM dyes, this suggest that the interactions between BR46 and the surface hydroxyl groups of the clay may be more weak than those between BM and the surface hydroxyl groups of the clay, that the chemical nature of adsorption can be occurred [29].

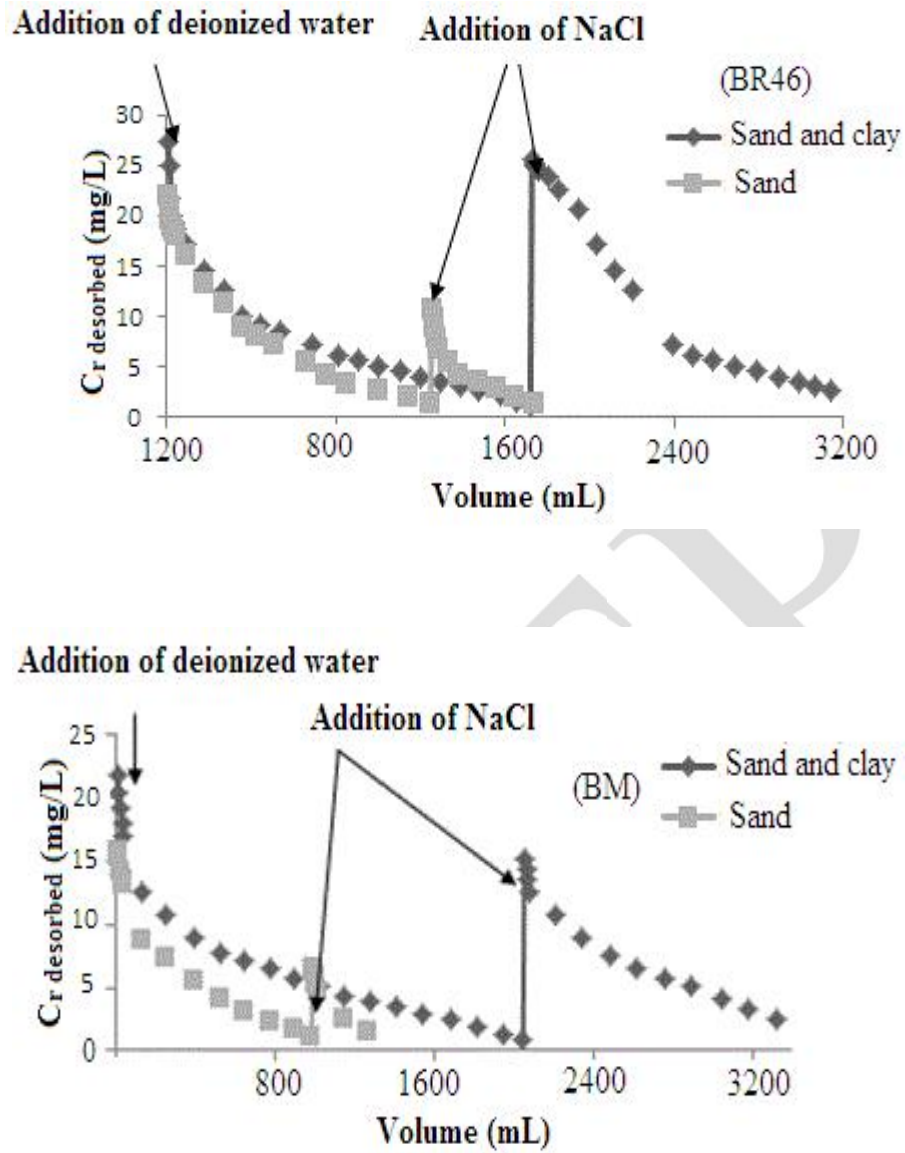


Fig. 5. Sand and the mixture (sand and clay) desorption using ultrapure water and NaCl solution (0.5 M) ($C_{\text{initial}} = 210 \text{ mg/L}$, Z: 20 cm, mass of clay: 3 g, mass of sand: 100 g, T: $25^\circ \pm 2^\circ \text{C}$).

4. CONCLUSION

Fixed-bed column study was conducted to find out the effectiveness of natural adsorbent, Moroccan clay of Safi for BR46 and MB adsorption. The investigations suggested that the adsorbent is efficient for BR46 and MB removal from water. The adsorption of these cationic dyes in a fixed-bed of mixed clay and sand was strongly dependent on the initial dyes concentration, flow rate and the bed height.

It was found that the breakthrough time decreases with the increasing initial concentration and flow rate, but it increases with increasing bed height. The performances of the fixed-bed columns were determined by the Bohart- Adams, the BDST models, and the Clark one. The breakthrough curves were well described by the Clark model at the ratios of C_t/C_0 higher than 0.4. The curve modelling using Bohart and Adams, describes the experience in the field of low concentrations, all of these models are found suitable for describing the dynamic behaviour of the column. The desorption studies of MB and BR46 have also been investigated at 210 mg/L, the interactions between BR46 and the surface hydroxyl groups of the clay may be more weak than those between BM and the surface hydroxyl groups of the clay, the adsorption may be chemical in nature. In conclusion, Moroccan clay of the Safi adsorbent, which is abundant and easily used, shows that it could be a promising adsorbent able to eliminate the cationic textile, it has a low desorption percentage, which promote the use of clay saturated with dyes in the ceramics industry and decoration products.

Acknowledgements

Authors acknowledge the research grant provided by the Cadi Ayyad University, High school of Technology, Faculty of Sciences Semlalia professors.

References

1. S K. Sharma and R. Sanghi (Eds) Advances in Water Treatment and Pollution Prevention, Springer (2012).
2. E. Alver, U. Metin Ays egul, J. Chem. Engin. 200- 202 (2012) 59- 67
3. P C. Vandevivere, R Bianchi and W Verstraete, J. Chem. Technol. Biotechnol. 72 (1998) 289- 302.
4. T. Robinson, G McMullan, R Marchant and P Nigam, J. Bioressour. Technol. 77(2001) 247-255.
5. B.Cheknane, M.Baudu, J-P.Basly, O. Bouras, F. Zermane, J.Chem. Engin. 209 (2012) 7- 12
6. T.S.Anirudhan, M Ramachandran, , Process Safety and Environ. Prot., 95, (2015), 215- 225.
7. Y Xubiao , W Chaohai, W Haizhen , Separation and Purification Technology, 156, (2015), 489- 495

8. A. Bennani Karim, B Mounir, M Hachkar, M Bakasse and A Yaacoubi, J. Hazard. Mater. 168 (2009) 304-309
9. A. Bennani Karim., B Mounir, M Hachkar, M Bakasse, A Yaacoubi, J. Water and Science 23, (2010) 375-388.
10. A A. Ahmad and B H. Hameed, J. Hazard. Mater. 175 (2010) 298- 303.
11. A A. N. Florencio, G A. V. Melissa, G. C. d. S.Meuris, J. water process engineering 3 . (2014) 90- 97
12. A. Cabrera-Lafaurie Wilman, R. Román Félix, J. Hernández-Maldonado Arturo, J. Hazardous Materials 282, (2015) 174- 182.
13. R.P. Han, Y. Wang, X. Zhao, Y.F. Wang, F.L. Xie, J.M. Cheng and M.S. Tang, Desalination 245 (2009) 284- 297.
14. I.A.W. Tan, A.L. Ahmad and B.H. Hameed, Desalination 225 (2008) 13-28.
15. R Nafisur., F K.Mohammad, J. Water Process Engineering 9 (2016) 254- 266
16. M. Auta, B.H. Hameed, J. Chemical Engineering 237 (2014) 352-361
17. M.Auta, B.H. Hameed, Colloids and Surfaces B: Biointerfaces, 105 (2013), 199- 206.
18. V. Christian Taty-Costodes, H.Fauduet, C. Porte and Yuh-Shan Ho, J. Hazard. Mater., 123 (2005) 135-144)
19. F. Ferrero, J. Hazard. Mater. 142 (2007) 144- 152.
20. K. H. Chu, J. Hazard. Mater. 177 (2010) 1006- 1012.
21. M. Calero, F. Hernáinz, G. Blázquez, G. Tenorio, M.A. Martín-Lara, J.Hazard. Mat. 171 (2009) 886-893
22. D.O. Cooney, Adsorption design for wastewater treatment, Lewis Publishers, Boca Raton, 1999
23. D.M. Ruthven, Principles of adsorption and adsorption processes, Wiley, NY, 1984.
24. Z. Aksu, F. Gönen, Process Biochemistry 39 (2004) 599–613
25. G. Bohart and F.Q. Adams, J. Am. Chem. Soc., 42 (1920) 523–544.
26. G.Jyotsna, K.Krishna, R.Chitra, K. G.Vinod, J. Hazardous Materials B125 (2005) 211- 220.
27. M. Sahel, O. Ferrandon Dusart, Rev. Sc. Eau, 6 (1993) 63-80.
28. M C. S. Reddy, V. Nirmala J. Arabian. Chem. Available online 6 October 2014, In Press, Corrected Proof.
29. M-Q. Jiang, X-Y. Jin, X-Q. Lu, Z-L. Chen, Desalination 252 (2010) 33- 39.